**Proceedings of MNC2007**
**MicroNanoChina07**
**January 10-13, 2007, Sanya, Hainan, China**

# MNC2007-21034

# NEAR-FIELD RADIATION INTERACTION WITH MOLECULES IN OPTICAL MICROCAVITY

**Zhixiong Guo**
**Dept. of Mechanical and Aerospace Engineering**
**Rutgers, The State University of New Jersey**
**Piscataway, NJ 08854, USA**
**guo@jove.rutgers.edu**

**Haiyong Quan**
**Dept. of Mechanical and Aerospace Engineering**
**Rutgers, The State University of New Jersey**
**Piscataway, NJ 08854, USA**
**hyquan@eden.rutgers.edu**

## ABSTRACT

Evanescent radiation-molecule interactions in an optical microcavity device are characterized. The device is operated at whispering-gallery modes, and consists of a microcavity and a micro-waveguide coupled by a sub-micrometer air-gap. Under optical resonance, a strong evanescent field arises along the periphery of the circular resonating microcavity. This radiation will certainly interact with molecules inside the field and may induce changes in the resonant field. Such induced changes are investigated and its potential in the detection of single molecules is discussed.

## INTRODUCTION

Whispering-gallery modes (WGM) occur when light travels in a dielectric medium of circular geometry. After repeated total internal reflections (TIR) at the curvilinear boundary the electromagnetic field can close on itself, giving rise to resonances. If the resonating cavity is in the micrometer level, one obtains a very small mode volume and high finesse. In recent years optical microcavities and WGM phenomena have received increasing attention due to their high potential for the realization of cavity quantum electrodynamics,[1] microlasers,[2] narrow filters,[3] optical switching,[4] miniature biosensors,[5] and high resolution spectroscopy,[6] to name a few.

Radiative transfer can be described by photon transport theory and Maxwell electromagnetism. Maxwell electromagnetism[7, 8] is commonly used to describe radiation phenomena in micro/nanometer scale. Conventional thermal radiation transport in meso/macroscale is well summarized in the textbooks.[9, 10] Some specific criteria have been established to delineate the micro/nanoscale and the meso/macroscale radiation regimes.[11, 12] The increasing demand for smaller structures and devices opens up new opportunities and challenges in micro/nanoscale heat transfer.[13-16]

Near-field radiation plays an important role in nanoscale diagnostics, such as in scanning probe microscopy.[14] Evanescent radiation-molecule interactions provide novel concepts and innovative tools for the exploration of molecular world. Optical techniques for single molecule detection have recently attracted much attention in the field of life sciences. Optical methods in the far field cannot localize the dimension to better than the diffraction limit. To overcome this restriction, the near-field optical techniques are widely and successfully utilized to study the dynamic properties of biological molecules. One highly successful sample is near-field scanning optical microscopy (NSOM). Recent advances in NSOM in combination with fluorescence techniques have allowed for the imaging,[17] dynamics,[18] spectroscopy,[19, 20] and resonance-energy transfer[21] of single molecules. Direct molecular detection through WGM signals[5, 22] might be possible.

In this study, we will simulate the interaction of single nanoscale biomolecules with the evanescent radiation field in optical microcavities. The interaction is governed by Maxwell's equations which will be solved via the finite element method. For the sake of calculation, the simulation is two-dimensional and the biomolecules are assumed of circular geometry. The induced resonant condition changes, such as frequency shift and intensity variation, due to the molecule-radiation interaction will be the emphasis of this investigation. In addition, we will also verify the simulation model through intensive benchmark comparison with the predicted resonant conditions via either analytical method or other numerical method.

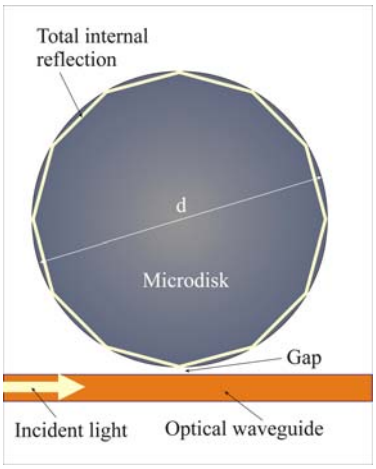


Figure 1. Sketch of a WGM microcavity.

## FORMULATION

The time-dependent Maxwell's equations are

$$\begin{cases} \nabla \cdot \bar{E} = \dfrac{\rho}{\varepsilon}; \quad \nabla \times \bar{E} = -\mu \dfrac{\partial \bar{H}}{\partial t} \\ \nabla \cdot \bar{H} = 0; \quad \nabla \times \bar{H} = \bar{J} + \varepsilon \dfrac{\partial \bar{E}}{\partial t} \end{cases} \tag{1}$$

where $\bar{E}$ and $\bar{H}$ are the electric and magnetic field vectors, respectively; $\varepsilon$ and $\mu$ are the permittivity and permeability of the medium; $\rho$ is the electric charge density; and $\bar{J}$ is the electric current density.

For the electric field, since $\rho = 0$ and $\bar{J} = \sigma \bar{E}$, we can derive the equation for $\bar{E}$ as follows:

$$\nabla^2 \bar{E} - \mu\sigma \frac{\partial \bar{E}}{\partial t} - \mu\varepsilon \frac{\partial^2 \bar{E}}{\partial t^2} = 0 \tag{2}$$

where σ is the electrical conductivity. We can transfer the above equation to the form of a time-harmonic wave by setting $\bar{E}(\bar{r},t) = \bar{E}_0(\bar{r})e^{i\omega t}$. The coupled set of Maxwell's equations is then reduced to a simple form:

$$\frac{1}{\mu}\nabla^2 \bar{E} + \omega^2 \varepsilon_c \bar{E} = 0; \quad \frac{1}{\mu}\nabla^2 \bar{H} + \omega^2 \varepsilon_c \bar{H} = 0 \tag{3}$$

where we have introduced the complex permittivity $\varepsilon_c = \varepsilon_{cr} \cdot \varepsilon_0 = \varepsilon - i(\sigma/\omega)$ and $\omega = 2\pi c/\lambda$; $c$ is the speed of light in the medium and $\lambda$ is the light wavelength. Here, the complex index of refraction, $m = n - ik$, is conveniently introduced for the treatment of wave propagation; $n$ is the real part of the refractive index and represents a spatial phase change of the electromagnetic wave; $k$ is the absorption index and stands for a spatial damping on the electromagnetic wave. The relationship between $\varepsilon_{cr}$ and $m$ is expressed by $\varepsilon_{cr} = m^2 = n^2 - k^2 - i2nk$.

In the present study we consider the In-plane TE waves, where the electric field has only a z-component; and it propagates in the x-y plane. WGM resonance inside a microdisk is typically an equatorial brilliant ring, and this ring is located on the same plane as the waveguide. For a planar microcavity device, it is may be feasible to use a two-dimensional (2-D) theoretical model. Thus, the fields can be written as:

$$\begin{aligned} \bar{E}(x,y,t) &= E_z(x,y)\bar{e}_z e^{i\omega t} \\ \bar{H}(x,y,t) &= [H_x(x,y)\bar{e}_x + H_y(x,y)\bar{e}_y]e^{i\omega t} \end{aligned} \tag{4}$$

At the interface and physical boundaries, the natural continuity condition is used. For the outside boundaries, the low-reflecting boundary condition is adopted. The low-reflecting means that only a small part of the wave is reflected, and that the wave propagates through the boundary almost as if it were not present. This condition can be formulized as $\bar{e}_z \cdot \bar{n} \times \sqrt{\mu}\bar{H} + \sqrt{\varepsilon}E_z = 0$. The light source term $E_{0z}$, which propagates inwards through the entry of the waveguide, was treated as an electrically low-reflecting boundary expressed by $\bar{e}_z \cdot \bar{n} \times \sqrt{\mu}\bar{H} + \sqrt{\varepsilon}E_z = 2\sqrt{\varepsilon}E_{0z}$.

The WGM resonances possess very high quality factors due to minimal reflection losses. The quality factor $Q$ is defined as a ratio of 2π stored energy to energy lost per cycle. From the energy conservation and resonance properties, we can deduce a simple approximate expression: $Q = \omega_0/\Delta\omega = 2\pi\omega_0\tau$, where $\omega_0$ is the resonant frequency, Δω is the resonance linewidth, and τ is the photon lifetime.

## RESULTS AND DISCUSSION

We consider an optical microcavity, coupled with a waveguide as shown in Fig. 1. The microdisk and waveguide are made of the same material (silicon nitride) and are assumed to have a constant refractive index of 2.01 against the excitation wavelengths. The surrounding medium is air. The gap is defined as the narrowest distance between the microdisk and the waveguide.

Versatile and accurate numerical approaches including the finite-difference time-domain (FDTD) method[23] and the finite element method[22, 24] (FEM) can be employed for solving the above mathematical models. The FEM is very flexible in terms of the treatment of irregular configurations such as the circular geometry of the microcavity. Thus, the In-plane TE waves application mode of the commercial FEMLAB package (version 3.0) was employed for the finite element analysis in the current calculations. The description of the numerical method is available in the literature; and thus, not repeated here. The accuracy of the FEM simulation is evaluated by validation studies through comparisons of FEM simulation results with corresponding analytical or published FDTD simulation results.

The numerically obtained resonance wavelength under the asymptotic limit, i.e., when the cavity is far away from the waveguide (the gap is larger than one optical wavelength), should be very close to the intrinsic resonance wavelength in a resonant mode for a given cavity. Through comparison of the simulated resonant wavelengths with the analytical results, it can verify the simulation model as well as its accuracy. Let's consider the intrinsic resonance wavelengths of a 2μm-diameter cavity.[24] The FEM simulation results are obtained when the gap is much larger than 1000nm. The intrinsic values were obtained through an analytical method[24] developed by us for analyzing resonance of an isolated cavity. Both the simulation and analytical results for various resonance modes are listed in Table 1 for comparison. It is obvious that the simulated results agree very well with the analytical results. The relative errors between the results are generally less than 0.2%. For example, the numerically obtained resonance wavelength at mode 12 is 822.964nm; while the corresponding intrinsic resonance wavelength is 822.9948nm. The relative error between these two values is 0.00374%. In Fig. 2, a comparison is further conducted between the E-fields predicted by the analytical and numerical methods, respectively. It is obvious that these two E-fields are very similar.

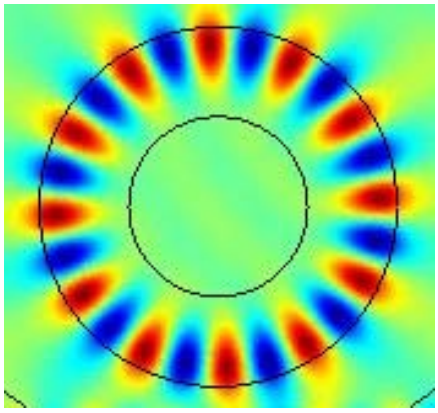

(a) FEM.

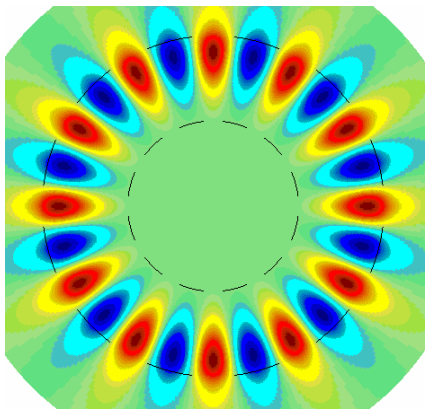

(b) Analytical.

Figure 2. Comparison of the E-fields of a 2μm-diameter cavity at resonant mode 12.

In the second validation study, our FEM model is used to simulate the resonance of a sample cavity demonstrated by Taflove and Hagness[23] using their FDTD simulation method. In both simulations, the calculation domain is a 6μm×7μm rectangular area. The microdisk resonator is 5μm in diameter and is coupled to two straight waveguides upon its top and below its bottom, respectively. The width of both waveguides is 300nm and the gap between the microdisk resonator and either waveguide is 232nm. The material of the microdisk and waveguides is GaAlAs, which has a refractive index of 3.2 for the considering wavelength range. The excitation light is introduced from the left end in the lower waveguide. The resonance frequencies of the radial mode numbers of 1, 2, and 3 with a same azimuthal mode number of 27 are listed in Table 2. Comparing the simulation results from FEM model with those from FDTD model, the relative error is about 0.12%. Furthermore, the E fields of those three cases and one off-resonance case obtained from the FEM and FDTD models are presented in Figs. 3 and 4 for comparison. It is seen that the E-field distributions at different modes illuminated by the both models are pretty similar.

.

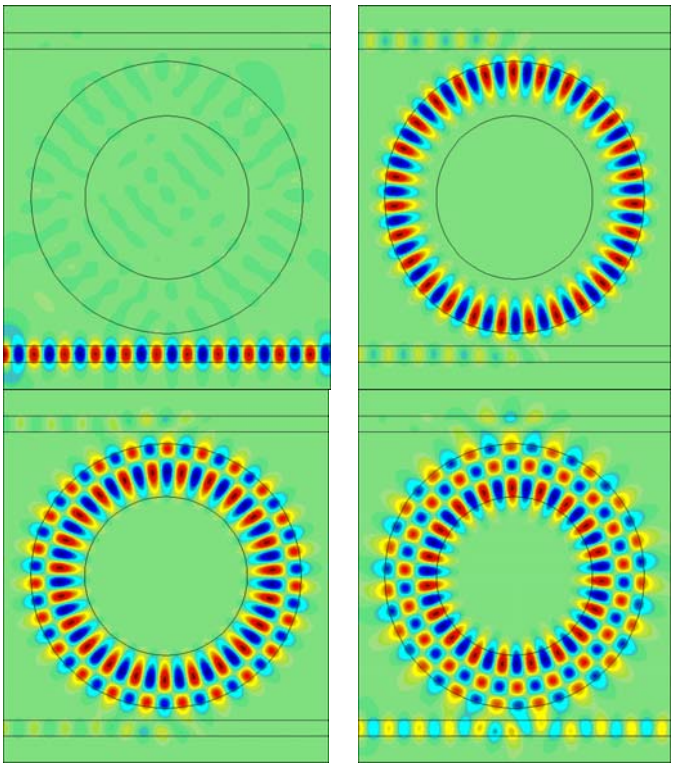

Figure 3. FEM predicted E-fields for a 5-μm-diameter microdisk: (Upper left) off-resonance with $f_0$ = 193.63THz, (Upper right) resonance radial mode 1 with $f_1$ = 189.42THz, (Lower left) resonance radial mode 2 with $f_2$ = 191.52THz, (Lower right) resonance radial mode 3 with $f_3$ = 188.04THz.

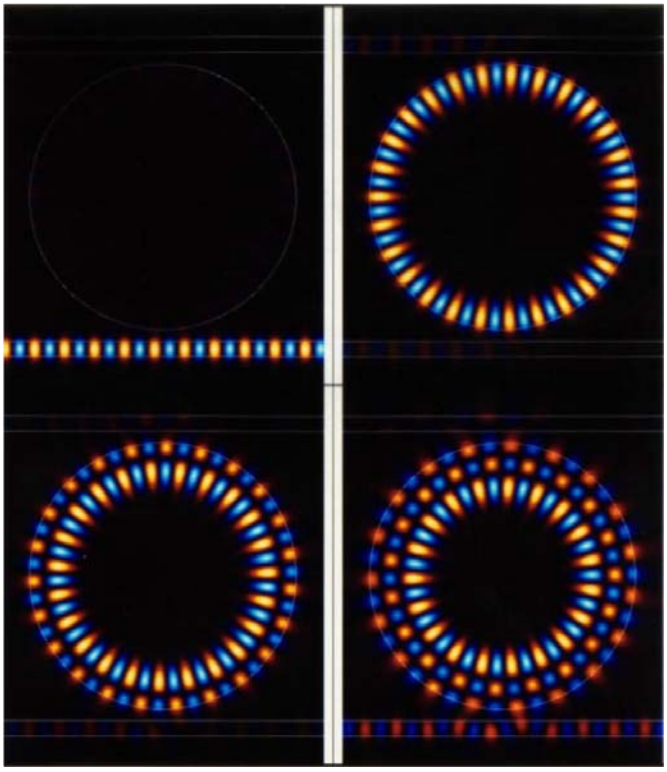

Figure 4. FDTD predicted E-fields for the 5-μm-diameter microdisk: (Upper left) off-resonance with $f_0$ = 193.4THz, (Upper right) resonance radial mode 1 with $f_1$ = 189.2THz, (Lower left) resonance radial mode 2 with $f_2$ = 191.3THz, (Lower right) resonance radial mode 3 with $f_3$ = 187.8THz (picture was copied from Taflove and Hagness[23]).

In conclusion, the accuracy of the FEM simulation model is validated by the excellent match of comparisons with the theoretical analysis and another numerical model.

Under the WGM first-order resonance, an exceedingly brilliant ring forms along the boundary of the microcavity.[22] Even though the incident light is very weak, the circulation overlapping inside the mode ring obviously enhances the mode intensity and provides the strong evanescent fields surrounding the resonator periphery surface. If single molecules are attached on the periphery or very close to this surface, molecule-evanescent field interactions occur. The interaction may result in resonance change inside the cavity.

In our previous study,[22] we demonstrated that a minor size change of a resonator due to uniform biomolecule binding would result in resonant frequency (or wavelength) shift. Now we suppose a single nanoscale molecule is approaching a resonator and investigate its effect on the resonances.

Let's consider a 2-μm-diameter microcavity with an approaching protein model molecule. In general, biomolecules have different shapes and sizes as well as different optical properties. Their refractive index varies in the range of 1.35-1.58.[25] In the present study, the shape of biomolecule phantoms is assumed to be circular and the molecular size discretely varies from 25nm to 550nm in diameter. Its refractive index is assumed to be 1.45, which is a typical value for proteins, without considering its absorption. The 2-μm-diameter microdisk has the first-order resonance mode (the azimuthal mode number is 12) at the wavelength of 802.93nm, in the case without any molecule attachment. The term of 'molecule attachment distance' (MAD) is used here to indicate the shortest distance between a molecule and the microdisk surface.

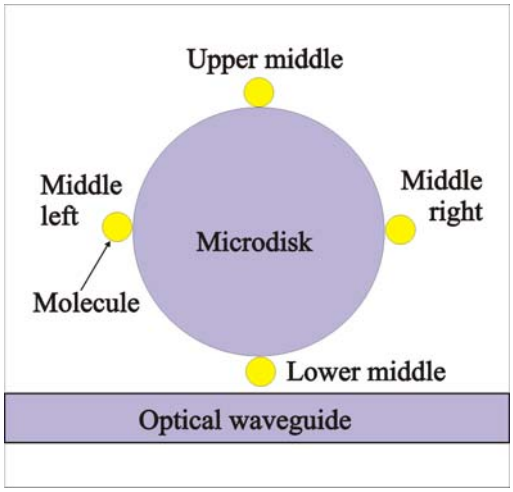


Figure 5. Schematic of a single molecule approaches to the periphery of a microcavity from four different locations.

First, we consider a single molecule of 200-nm in diameter is approaching to the periphery of the microcavity from four different orientations as shown in Fig. 5. Figure 6 shows the simulation data and exponentially fitted curve of the resonant wavelength shift (RWS) vs. the molecule attachment distance. The tiny fluctuation of the simulation data at different locations indicates that the molecule approaching direction effect is very small. On the other hand, this reveals that the electric field and the electromagnetic energy density distribution of the microdisk WGM resonance mode is axisymmetric. From Fig. 6, it is observed that the MAD obviously affects the value of RWS. The RWS from the attached molecule decays with increasing MAD in an exponential manner, and finally approaches to zero at about 500 nm MAD.

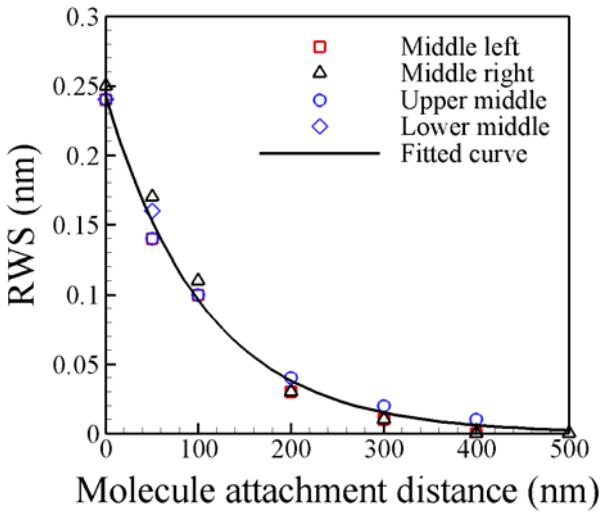


Figure 6. Induced resonance wavelength shifts due to an approaching single molecule of 200 nm in diameter.

The MAD also affects the radiation intensity of the resonance mode inside the microdisk. A molecule which is closer to the microdisk surface may absorb more energy from the resonance mode ring. Figure 9 shows the effects of a single molecule attachment on the E-field of the 2μm-diameter WGM resonator. The considered diameter of the molecule is 200 nm and 400 nm, respectively, for comparison. The single molecule is approaching the surface of the resonator with various MADs. From Fig. 9, it is seen that with decreasing MAD, the effect of single molecule attachment on the WGM becomes strong and strong.

Molecule size is another important parameter, that will influence not only the radiation intensity of resonance mode (as shown in the comparison of Fig. 7), but also the RWS for the resonance mode. In Fig. 8, the stored energy inside the microcavity drops with increasing molecular size, due to the enhancement of the near-field scattering surrounding the microcavity. The stored energy has a big drop when the molecular size increases from 25nm to 150nm, particularly if the MAD is less than 100 nm. The attachment condition is also a critical parameter to determine the intensity decay. For instance, the presence of a molecule of 500 nm in diameter at a MAD of 200 nm results in a reduction of 50% stored energy, whereas the same molecule at 0-nm MAD condition reduces the stored energy by 90%.

The present study reveals that, by monitoring the WGM signal changes (such as RWS and intensity), it is possible to detect single molecules and/or follow up molecular events. These can be used for designing new biomolecular sensors.

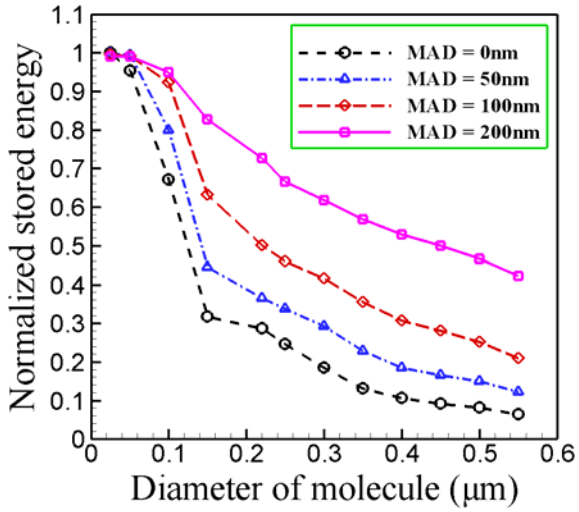


Figure 8. Single molecule size effect on the stored energy inside the microcavity.

## CONCLUSION

Whispering-gallery mode optical resonances and molecule-radiation interactions were simulated using the finite element solution of Maxwell's equations. First the FEM simulation model was verified. Excellent agreements were found between the FEM simulation and analytical results for an isolated resonator, and between the FEM and published FDTD simulation for a microcavity coupled with two waveguides.

The influence of molecular attachment is investigated. It is found that the presence of a single molecule will affect the resonance field intensity and result in a resonance frequency shift. The location of attachment is not important. However, the molecule size and attachment distance are two key parameters. With decreasing attachment distance or increasing molecule size, the shift of resonance frequency increases and the resonance field intensity becomes weak.

Detection of single molecules is possible through measurement of the WGM signal changes due to molecule-radiation interactions. The interaction could alter the signal intensity and shift resonant frequencies. The molecule attachment distance as well as the molecule properties and size will all affect the WGM signals. More in-depth studies are needed in order to fulfill the goal of WGM-based direct molecular sensing.

## ACKNOWLEDGMENTS

Z. Guo is grateful to the support of the Academic Excellence Fund Awards (2003-2004, and 2005-2006) from

Rutgers University and a grant from the National Science Foundation (CTS- 0541585) to the project.

## REFERENCES


1. K. J. Vahala, "Optical microcavities", *Nature* **424**, 839-846 (2003).
2. M. Cai, Q. Painter, K.J. Vahala, and P. C. Sercel, "Fiber-coupled microsphere laser", *Opt. Lett.*, **25**, 1430-1432 (2000).
3. B. E. Little, S. T. Chu, H. A. Haus, J. Foresi, and J. P. Laine, "Microring resonator channel dropping filters", *J. Lightwave Tech.* **15**, 998-1005, (1997).
4. F. C. Blom, D. R. van Dijk, H. J. Hoekstra, A. Driessen, and T. J. A. Popma, "Experimental study of integrated-optics micro-cavity resonators: toward an all-optical switching device," *Appl. Phys. Lett.* **71**, 747-749, (1997).
5. S. Arnold, M. Khoshsima, I. Teraoka, and F. Vollmer, "Shift of whispering-gallery modes in microspheres by protein adsorption", *Opt. Lett.* **28**, 272-274 (2003).
6. S. Schiller, and R. L. Byer, "High-resolution spectroscope of whispering gallery modes in large dielectric spheres," *Opt. Lett.* **16**, 1138-1140 (1991).
7. C. F. Bohren, and D. R. Huffman, *Absorption and Scattering of Light by Small Particles*, John Wiley and Sons, New York (1983).
8. G. Chen, "Wave effects on radiative transfer in absorbing and emitting thin-film media", *Microscale Thermophysical Eng.* **1**, 215-224 (1997).
9. Siegel R., and Howell J.R., *Thermal Radiation Heat Transfer*, 4th ed., Taylor & Francis, New York (2001).
10. M. F. Modest, *Radiative Heat Transfer,* 2nd ed., Academic Press, New York (2003).
11. S. Kumar, "Thermal radiation transport in micro-structures", *Thermal Science and Engr.* **2**, 149-157 (1992).
12. C. L. Tien, A. Majumdar and F. M. Gerner, *Microscale Energy Transport*, Taylor & Francis, Washington, DC (1997).
13. G. Chen, 1996, "Heat transfer in micro- and nanoscale photonic devices," *Annual Review of Heat Transfer*, Ed., C.L. Tien, Vol. VII, 1-57 (1996).
14. A. Majumdar, "Scanning Thermal Microscopy", *Annu. Rev. Mater. Sci*. 29, 505-585 (1999).
15. C.P. Grigoropoulos, S. Moon, M. Lee, M. Hatano and K. Suzuki, "Thermal transport in melting and recrystallization of amorphous and polycrystalline Si thin films," *Applied Physics A* **69** (supplement), S295-S298 (1999).
16. X. Wang, and Xu, X., "Nanoparticles Formed in Picosecond Laser Argon Crystal Interaction," *J. Heat Transfer* **125**, 1147-1155 (2003).
17. A.J. Meixner, D. Zeisel, M.A. Bopp, and G. Tarrach, "Super-resolution imaging and detection of fluorescence from single molecules by scanning near-field optical microscopy," *Opt. Eng*. **34**, 2324-2332 (1995).
18. X.S. Xie and R.C. Dunn, "Probing single molecule dynamics," *Science* **265**, 361-364 (1994).
19. J.K. Trautman, J.J. Macklin, L.E. Brus, and E. Betzig, "Neal-field spectroscopy of single molecules at room temperature," *Nature* **369**, 40-42 (1994).
20. D. Siegberg, C.M. Roth, D.P. Herten, "Single molecule fluorescence spectroscopy – Approaches towards quantitative investigation of structure and dynamics in ling cells," *Proc. of SPIE* **6092**, 609202 (2006).
21. T. Ha, T. Enderle, D.F. Ogletree, D.S. Chemla, P.R. Selvin and S. Weiss, "Probing the interaction between two single molecules: fluorescence resonance energy transfer between a single donor and a single acceptor," *Proc. Natl. Acad. Sci.* **93**, 6264-6268 (1996).
22. H. Quan and Z. Guo, "Simulation of whispering-gallery-mode resonance shifts for optical miniature biosensors," *J. Quantitative Spectroscopy & Radiative Transfer* **93**, 231 – 243 (2005)
23. A. Taflove and S. C. Hagness, *Computational Electrodynamics: The Finite-Difference Time-Domain Method*, 2nd ed., Artech House, Norwood, MA (2000).
24. H. Quan, "Characterization of optical whispering gallery mode resonance and applications", Ph.D. dissertation, Rutgers University (2006).
25. Http://www.nmr.mgh.harvard.edu/~adunn/papers/dissertation/node7.html.

| Azimuthal mode number n | 8 | 10 | 12 | 14 |
|---|---|---|---|---|
| Theoretical RW(nm) | 1170.548 | 964.891 | 822.9948 | 718.755 |
| Numerical RW(nm) | 1168.9 | 964.11 | 822.964 | 718.709 |
| Relative error (%) | 0.14079 | 0.08094 | 0.00374 | 0.00640 |
| Azimuthal mode number n | 16 | 18 | 20 | 22 |
| Theoretical RW(nm) | 638.6908 | 575.1338 | 523.3831 | 480.2857 |
| Numerical RW(nm) | 638.638 | 575.067 | 523.2915 | 480.2722 |
| Relative error (%) | 0.00827 | 0.01161 | 0.0175 | 0.00281 |

Table 1. Comparison of the theoretical and simulated resonance wavelengths for a 2μm-diameter cavity.

| Radial mode number | 1 | 2 | 3 |
|---|---|---|---|
| FDTD model (THz) | 189.2 | 191.3 | 187.8 |
| FEM model (THz) | 189.42 | 191.52 | 188.04 |
| Relative error | 0.12% | 0.12% | 0.13% |

Table 2. Comparison of resonance frequencies between the predictions of FEM and FDTD (data were cited from Taflove and Hagness[23]).

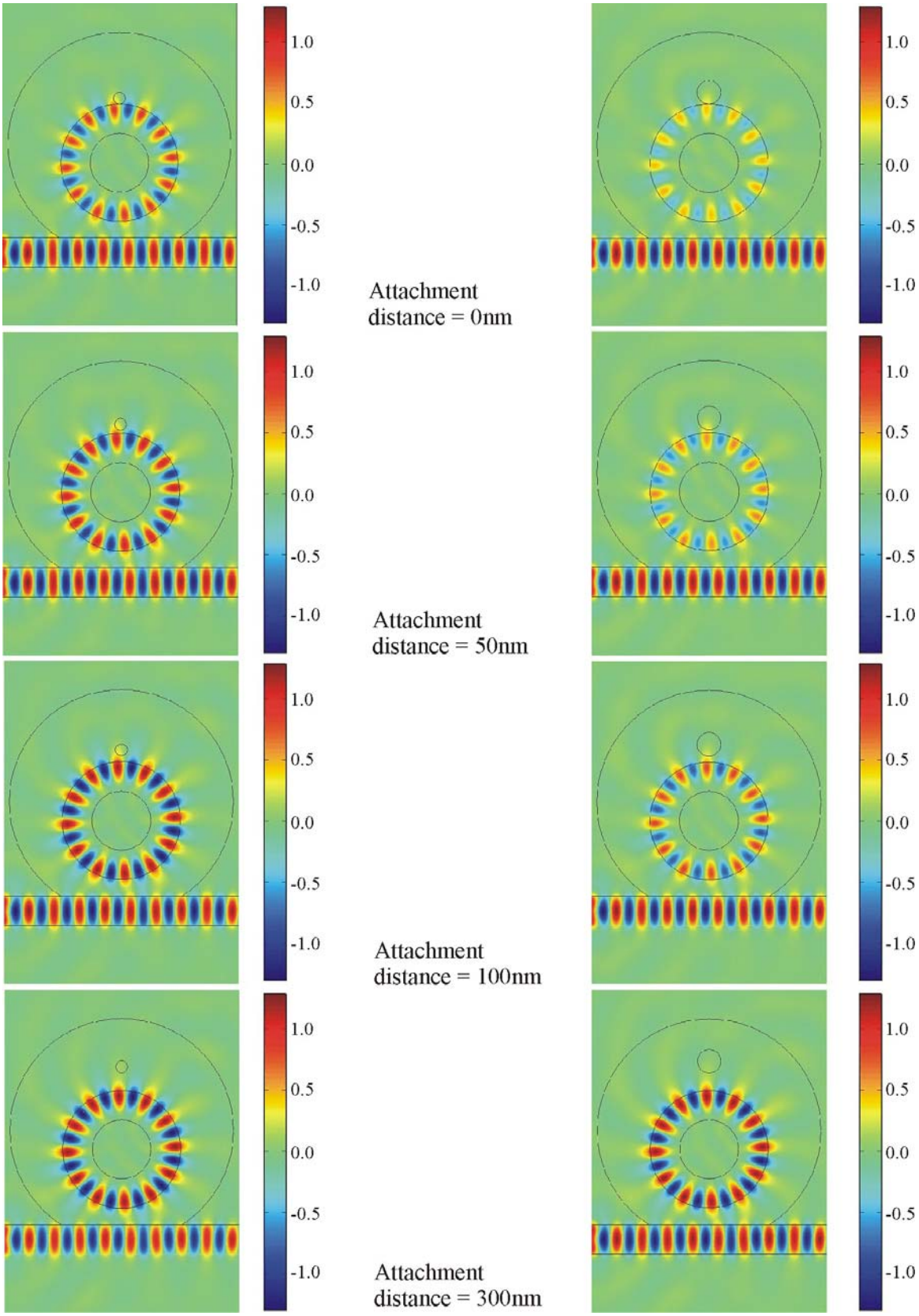


Figure 7. Effects of a single molecule attachment on the WGM resonance: (a) diameter of the molecule = 200nm; (b) diameter of the molecule = 400nm.